pubs.acs.org/acschemicalbiology

Letters

Probing the KRas Switch II Groove by Fluorine NMR Spectroscopy

D. Matthew Peacock, Mark J. S. Kelly, and Kevan M. Shokat*

Cite This: *ACS Chem. Biol.* 2022, 17, 2710–2715

Read Online

ACCESS | Metrics & More | Article Recommendations | Supporting Information

ABSTRACT: While there has been recent success in the development of $KRas^{G12C}$ inhibitors, unmet needs for selective inhibitors of $KRas^{G12D}$ and the remaining oncogenic KRas proteins remain. Here, we applied trifluoromethyl-containing ligands of KRas proteins as competitive probe ligands to assay the occupancy of the switch II pocket by ^{19}F NMR spectroscopy. Structure–activity-relationship studies of probe ligands increased the sensitivity of the assay and identified structures that differentially detected each nucleotide state of $KRas^{G12D}$. These differences in selectivity, combined with the high resolution of ^{19}F NMR spectroscopy, enabled this method to be expanded to assay both nucleotide states of the protein simultaneously.

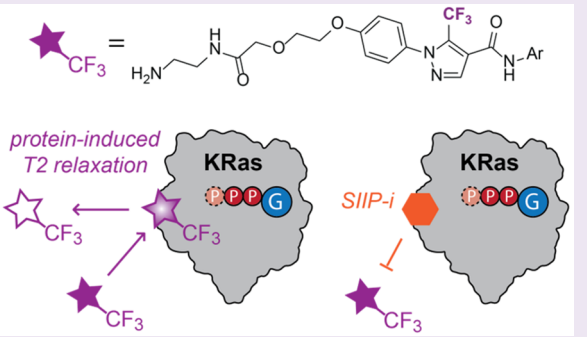

INTRODUCTION

The proto-oncogene *KRAS* is among the most frequently mutated genes in human cancers, with mutations found in approximately 14% of patient samples.[1] Its protein product (KRas) is a membrane-localized small GTPase responsible for cell growth and proliferation signaling through its effectors RAF and PI3K.[2] Transforming mutations in *KRAS* (most commonly at G12, G13, or Q61) result in an increased cellular proportion of active GTP-bound KRas, typically by impairing the hydrolysis reaction of GTP.

Recent drug discovery campaigns relying on covalent chemistry have resulted in the first FDA-approved *KRAS* inhibitor sotorasib (AMG510), which selectively targets KRas proteins containing a G12C mutation.[3−12] Sotorasib has weak reversible affinity to a cryptic pocket on the protein, termed the switch II-pocket (SIIP), and relies on an irreversible covalent reaction with the mutant cysteine for its affinity and selectivity. In contrast, adagrasib (MRTX849) bears a weaker electrophile but possesses stronger reversible affinity to the same SIIP binding site (K_i = 4 μM).[13] Further structure–activity relationship (SAR) studies of the adagrasib scaffold led to MRTX1133, the first cell-active $KRas^{G12D}$ SIIP inhibitor, in which the noncovalent interactions were optimized to achieve subpicomolar binding affinity.[14] Despite these recent successes, selective inhibitors for the protein products of many *RAS*-family oncogenes are still unknown, and occupancy probes which can report on ligand binding to the GDP-OFF and GTP-ON states of Ras proteins are limited.

Protein-observed nuclear magnetic resonance (NMR) spectroscopy has proven to be a powerful tool in drug discovery generally and in the study of KRas protein–ligand interactions specifically.[15−17] Furthermore, the two nucleotide states of KRas can be resolved by protein-observed NMR spectroscopy, enabling nucleotide-cycling reactions and nucleotide-state-specific binding to be directly observed in mixed samples containing both GDP and GTP.[18−21] While information-rich, protein-observed experiments are burdened by the requirements of high protein concentrations, long acquisition times, and isotopic labels. Ligand-observed NMR spectroscopy alleviates these burdens; well-validated "probe" ligands can be applied to assay properties of the protein at lower concentrations, with faster acquisition times, and without the need for isotopic labeling.

In this study, we applied trifluoromethyl-containing ligands to the KRas switch II groove as probes to assay KRas proteins in both nucleotide states by ^{19}F NMR spectroscopy. One-dimensional ^{19}F Carr–Purcell–Meiboom–Gill (CPMG1D) experiments were used to detect changes in the probes' rates of transverse relaxation resulting from binding to the KRas protein. These probes were applied to assay competitive binding by SIIP-targeted inhibitors such as MRTX849, MRTX1133, and the cyclic peptide KD2.

RESULTS AND DISCUSSION

Reversible Binding to the Switch II Groove Is Observed by NMR Spectroscopy. We considered that a suitable probe structure to assay the switch II pocket of KRas proteins by ligand-observed NMR spectroscopy would have the following characteristics: (1) short residence time and weak affinity (K_D 10^{-3} to 10^{-5} M) to enable averaging of

Received: July 12, 2022
Accepted: September 2, 2022
Published: September 27, 2022

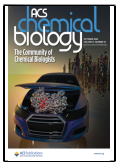

https://doi.org/10.1021/acschembio.2c00566
ACS Chem. Biol. 2022, 17, 2710–2715

bound and unbound populations, (2) affinity for each of the two nucleotide states, and (3) an appropriate NMR handle to enable sensitive detection of the probe molecule under dilute conditions (≤100 μM). A previously reported disulfide-tethering screen against a KRas mutant containing an engineered cysteine (M72C) yielded a fragment (2C07, **1**; Figure 1A) that we considered likely to serve as a starting point for ligand design to meet these requirements.[22] This fragment occupied a site known as the switch II groove (SIIG), lying along a shallow lipophilic channel formed between α3 and SII. This disulfide fragment (**1**) and an acrylamide derived from it (**2**) reacted with KRas^{M72C} in both its inactive state (bound to GDP) and its active state (bound to GNP, a nonhydrolyzable GTP analog). Furthermore, the trifluoromethylpyrazole moiety in these compounds is an ideal structure for ligand-observed ^{19}F NMR techniques; the three equivalent fluorines are observed as a strong singlet without any significant J-coupling due to the absence of nearby spin-active nuclei. The lack of biological fluorines greatly simplifies the analysis of ^{19}F NMR spectra of protein−ligand mixtures when compared to ^{1}H NMR spectra.[23] However, the reversible affinities of these compounds to proteins lacking the M72C mutation were unconfirmed.

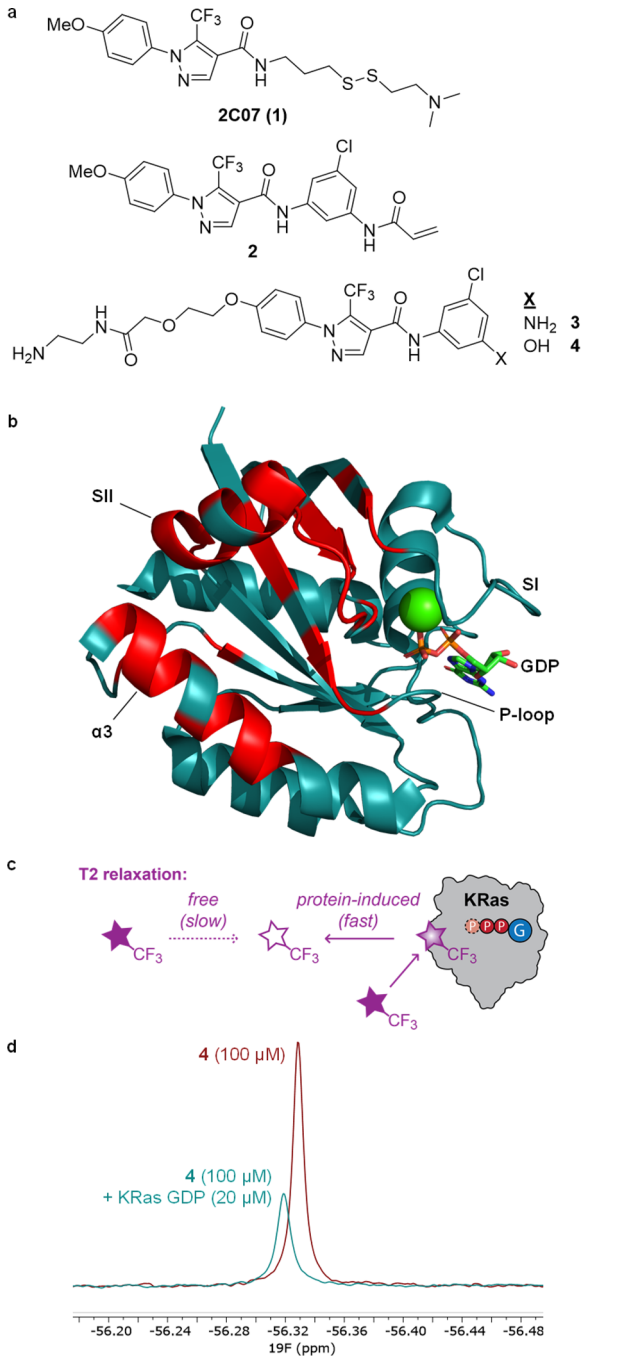

Figure 1. Solubilized derivatives of 2C07 bind the KRas SIIG. (a) Chemical structures of SIIG binders. (b) Top (>1σ) CSPs caused by **4** marked in red on KRas GDP structure 4LPK. (c) Cartoon depiction of KRas-induced T2 relaxation in a probe ligand. (d) ^{19}F CPMG NMR spectra (160 ms) of **4** in the absence (red) and presence (cyan) of KRas GDP.

Acrylamide **2** has very low aqueous solubility, and initial investigations of its reversible affinity were hindered by the formation of aggregates. To improve the solubility of **2**, the solvent-exposed methyl ether was extended into a polar solubilizing tail. The acrylamide was removed because oncogenic KRas proteins do not possess the engineered M72C mutation. These modifications resulted in compounds **3** and **4** (Figure 1A). Binding of **3** or **4** uniformly to ^{15}N-labeled KRas^{WT} and KRas^{G12D} GDP 1−169 was observed by HSQC NMR spectroscopy, and perturbed peaks were mapped onto the previously determined structure of KRas GDP (Figure 1B, Figure S1, PDB 4LPK). The largest of these perturbations are in the SII and α3 regions, which is consistent with expectations based on the structure of the KRas^{M72C}-**1** GDP complex (PDB 5VBM).[22] Smaller perturbations were observed in the P-loop and in switch I (SI)—outside the expected binding site—likely due to conformational change in these dynamic regions. However, the reversible affinities of **3** and **4** were very weak; a 1 mM concentration of either ligand did not saturate the binding site (Figure S1C).

Ligand-Observed CPMG NMR Spectroscopy Detects Oncogenic KRas Mutant Proteins. We then sought to determine whether these SIIG-binders could serve as probe ligands to detect KRas proteins by ^{19}F NMR spectroscopy. One-dimensional CPMG experiments [90-(τ-180-τ)$_n$], in which a spin−echo with delay τ is looped n times, attenuate signal intensity as a function of the transverse relaxation rate (R_2) and total spin echo time ($2\cdot\tau\cdot n$). Prior studies have shown that reversible binding of proteins to fluorine-containing small molecules induces an increase in the observed ^{19}F R_2 at long values of τ, which maximize the exchange contribution to R_2.[24,25] Applying a 160 ms (τ = 20 ms, n = 4) CPMG filter to the ^{19}F NMR spectrum of **4** (100 μM) in the presence of KRas GDP 1−169 resulted in a decrease in the measured integral (I) compared to the same spectrum acquired in the absence of protein (I_0) (Figure 1C,D). However, these experiments required a relatively high concentration (20 μM) of protein to significantly reduce the integral of **4**. Further modifications to the probe structure were required to improve its binding affinity and the sensitivity of the ^{19}F CPMG NMR assay.

To improve the sensitivity of this method for oncogenic KRas proteins and to explore the relationship between structure and nucleotide-state specificity, we synthesized a series of derivatives of **3** and **4** with varied structure at the aryl ring expected to be buried deepest within the pocket, and these derivatives were evaluated by CPMG NMR spectroscopy against both nucleotide states of KRas^{G12D} (6 μM; Figure 2A,B). From this series, five compounds (**9**, **12**, **14**, **15**, and **17**) showed increased sensitivity compared to **3** and **4**.

https://doi.org/10.1021/acschembio.2c00566
ACS Chem. Biol. 2022, 17, 2710−2715

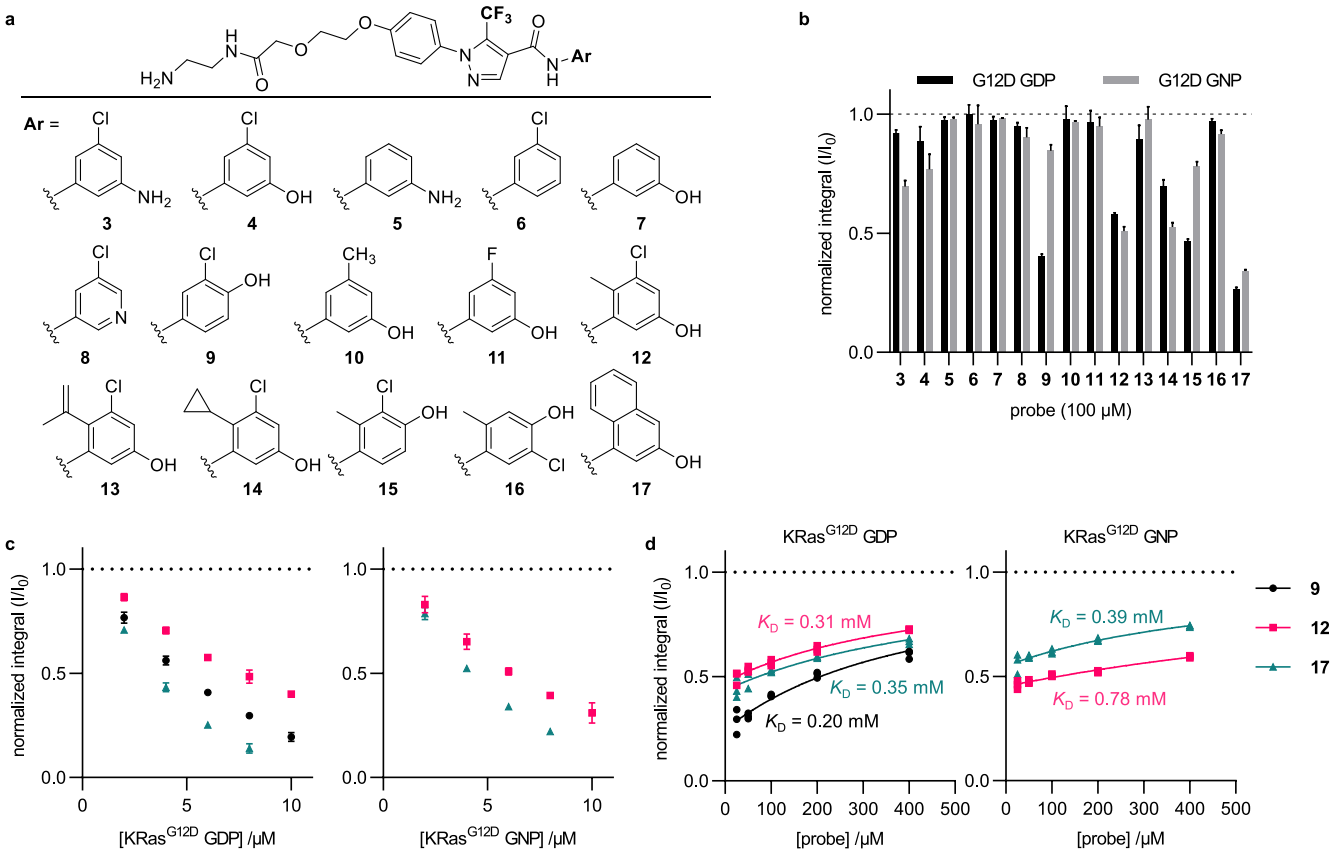

Figure 2. SAR of SIIG binders enables more sensitive detection of KRas^{G12D}. (a) Chemical structures of SIIG binders. (b) Normalized integrals (I/I_0) from ^{19}F CPMG NMR spectra (160 ms) of probes (100 μM) with KRas^{G12D} (6 μM); values are means ± errors propagated from SD (n = 3). (c) Effect of varying KRas^{G12D} concentration on I/I_0; values are means ± errors propagated from SD (n = 3). (d) Effect of varying probe concentration on I/I_0; $[P]_0$ = 6 μM for probes **9** and **12**, 3 μM for probe **17**; individual points shown (n = 3); data fit to eq 1 (SI).

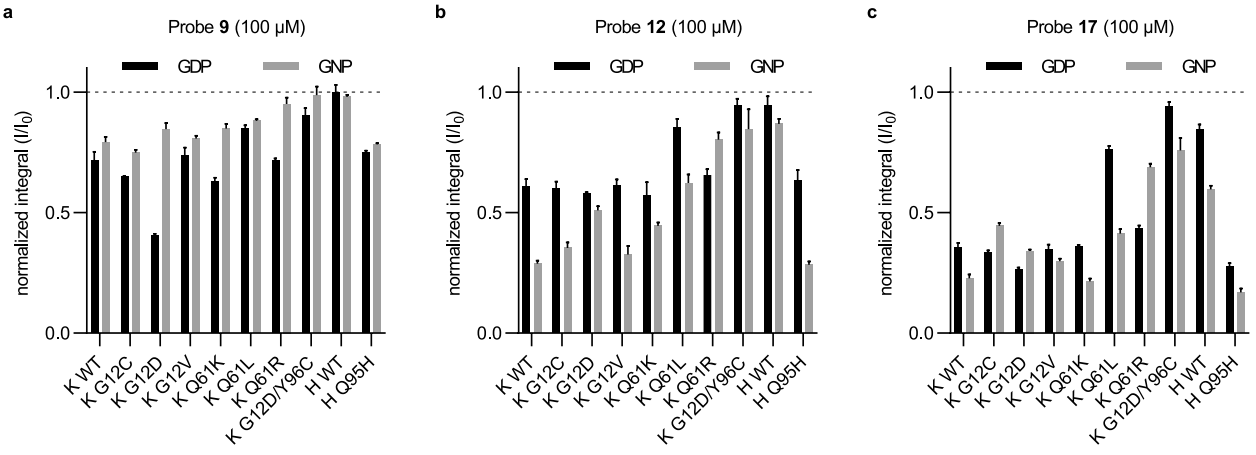

Figure 3. ^{19}F CPMG NMR spectroscopy detects a variety of oncogenic KRas proteins. Normalized integrals (I/I_0) from ^{19}F CPMG NMR spectra (160 ms) of 100 μM **9** (a), **12** (b), or **17** (c) in the presence of 6 μM KRas or HRas proteins; values are means ± errors propagated from the SDs of I and I_0 (n = 3).

Compound **9**, an isomer of **4** in which the hydroxy group is attached at C-4 of the aryl ring, specifically detected the GDP state of KRas^{G12D}. Compounds **12**, bearing a methyl group at C-2, and **17**, in which the phenyl ring is replaced by a naphthyl, detected both nucleotide states with similar sensitivity. Probe **9** relaxed more slowly in the absence of protein ($R_{2,free}$ = 2.4 Hz) than did compounds containing the C-5 hydroxy group ($R_{2,free}$ = 6.3 Hz for **4**, 4.4 Hz for **12**, and 5.0 Hz for **17**), increasing the sensitivity and dynamic range of integral measurements with this probe (Figure S2). Furthermore, probe **9** was confirmed to be a tighter binder to the SIIG of U−^{15}N KRas^{G12D} GDP by HSQC NMR compared to **4** (Figure S3).

The probe and protein concentrations were varied to determine the dependence on each binding partner. The normalized integrals (I/I_0) of the probes decreased exponentially with increasing protein concentrations (Figure 2C, Figure S2C,D). The normalized integrals increased with increasing probe concentrations, and K_D values for the probe−protein

https://doi.org/10.1021/acschembio.2c00566
ACS Chem. Biol. 2022, 17, 2710−2715

binding were extracted by fitting the data to eq 1 (Figure 2D, SI). Probe **9** bound the GDP state more strongly than did probes **12** or **17** (**9**K_D = 0.20 mM); however, we did not observe a clear correlation between these three probes' binding affinities and sensitivities to detect KRas^{G12D} proteins.

Probes **9**, **12**, and **17** were evaluated against both the inactive GDP and active GNP nucleotide states of a panel of KRas proteins (three common mutations at G12 and three common mutations at Q61) to determine whether this method can be generalized across the protein products of the most frequent *KRAS* oncogenes (Figure 3). Probe **9** most sensitively detected the GDP state of KRas^{G12D} and more weakly detected the remaining oncogene products excepting KRas^{Q61R} GNP (Figure 3A). Probes **12** and **17** detected both nucleotide states of all oncogene products tested, albeit with weaker sensitivity for KRas^{Q61L} GDP and KRas^{Q61R} GNP than for the others (Figure 3B,C). The closely related protein HRas 1−166 contains only one residue difference within the SIIG binding site (Q95 in HRas vs H95 in KRas). HRas was only weakly detected by this method; however, the results with HRas^{Q95H} closely matched those obtained with KRas^{WT}. Similarly, a recently identified mutation that confers resistance to adagrasib (Y96C) greatly weakened detection of KRas^{G12D}.[26]

SIIP-Targeted Inhibitors Competitively Displace SIIG-Targeted ^{19}F NMR Probes. Having identified probe ligand structures that detected low micromolar concentrations of KRas proteins, we next sought to determine whether these probes could assay competitive reversible binding of ligands within or adjacent to the SIIG. Since the SIIG and SIIP are overlapping binding sites, we expected binding to either of them to be mutually exclusive (Figure S4A). We measured the effect of MRTX849 on the normalized integral of probe **9** (100 μM) in the presence of KRas^{G12D} GDP (2 μM; Figure 4A,B). MRTX849 displaced probe **9**, and the calculated fraction occupancy data were fit to eqs 3 and 4 (SI) to extract the K_i of MRTX849 (2.9 μM). This result agrees well with the affinity expected based on kinetic data from its reaction with KRas^{G12C}.[13] In contrast, two G12C-targeted inhibitors based on different scaffolds (AMG510 and JDQ443) did not occupy the SIIP of KRas^{G12D} when tested at 60 μM (Figure S4B,C).

Recognition of the two nucleotide states of KRas proteins is a key property of inhibitors, relating both to an inhibitor's mechanism of action and its ability to access constitutively active proteins. We sought to determine whether this ^{19}F NMR method could be extended to assay the nucleotide state of KRas^{G12D} and the nucleotide-state specificity of SIIP inhibitors. Since their resonances are resolved, and neither ligand saturates the binding site, the transverse relaxation rates of **9** and **12** could be measured simultaneously in a mixture. We tested whether this combination of probes could discriminate between the inactive GDP state and the active and inactive conformations of the GTP state. The transverse relaxation rate of probe **9** exhibited a strong dependence on the nucleotide state and conformation of KRas^{G12D}; $R_{2,9}$ varied over 6 Hz between samples containing 6 μM of either KRas^{G12D} GDP, KRas^{G12D} GNP, KRas$^{G12D/T35S}$ GNP (state 1 inactive conformation), or KRas^{G12D} GNP + RAF1-RBD 52−131 (state 2 active conformation; Figure S4D). Meanwhile, $R_{2,12}$ varied relatively little (<2 Hz) among the same samples.

From these data, equations to calculate the individual concentrations of the GDP and GNP states in a mixture were determined (eqs 5 and 6, SI, Figure S4D,E). Addition of the moderate-affinity binder MRTX849 (60 μM, GDP-state K_i = 2.9 μM) selectively occupied the GDP state of the protein (Figure 4C). The high-affinity binder MRTX1133 (GDP-state K_i < 1 pM) occupied both nucleotide states when added in excess (15 μM). However, substoichiometric quantities (2, 4, and 6 μM) of MRTX1133 selectively occupied the GDP-state, consistent with the previously reported high GDP-state selectivity of a closely related structure.[21] In contrast to the small molecule SIIP binders, the cyclic peptide KD2 preferentially occupied the active GNP state.[27]

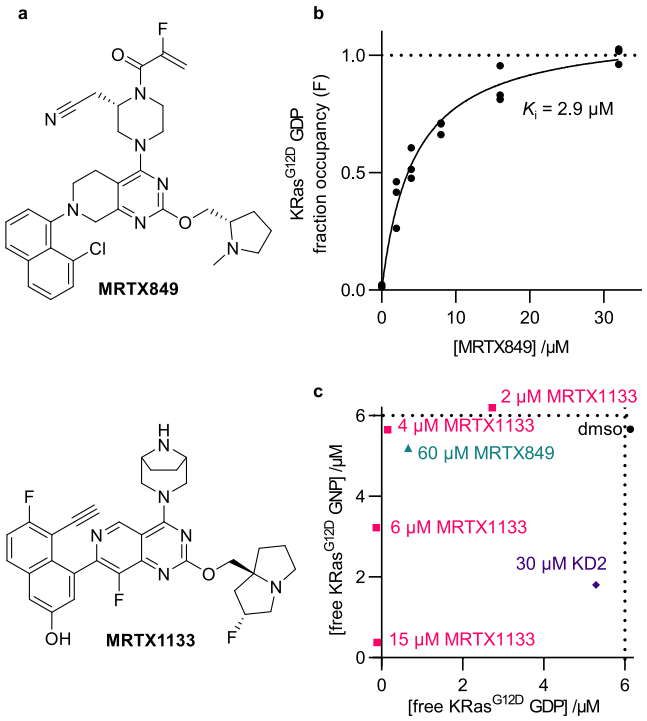

Figure 4. SIIP inhibitors compete with SIIG probes. (a) Chemical structures of MRTX849 and MRTX1133. (b) Fraction occupancy (F) of MRTX849 binding to KRas^{G12D} GDP (2 μM) calculated from ^{19}F CPMG NMR spectra (320 ms) of **9** (100 μM) according to eqs 2−4 (SI); individual points shown (n = 3). (c) Simultaneous monitoring of both nucleotide states of KRas^{G12D} (6 μM each) with a mixture of **9** and **12** (50 μM each); concentrations were calculated with eqs 5 and 6 (SI) from the means of R_2 measurements (n = 2−4).

CONCLUSIONS

We have synthesized trifluoromethyl-containing ligands that bind to the SIIG of KRas proteins in both nucleotide states, and we have shown that these compounds serve as ^{19}F NMR spectroscopy probes for a variety of oncogenic KRas proteins. SAR studies identified modifications in the probe structure to improve the sensitivity and nucleotide-state selectivity of the assay. The probes were stoichiometrically competed by SIIP-targeted inhibitors, enabling their use to quantify the occupancy of the SIIP.

While many biochemical methods to assay competitive binding between two ligands are known, few allow simultaneous interrogation of two closely related proteins in a single sample, such as the two nucleotide states of KRas. Knowledge of the nucleotide-state selectivity of SIIP inhibitors is likely important to understand their cellular engagement of constitutively activated KRas proteins, but current methods to directly query this selectivity are lacking. The method and probe ligands reported in this work enable the approximation

https://doi.org/10.1021/acschembio.2c00566
ACS Chem. Biol. 2022, 17, 2710−2715

of the occupancy of both nucleotide states from a single sample, allowing an inhibitor's nucleotide-state selectivity to be assayed in a competitive manner.

The probe ligands described in this work can be used to detect KRas proteins at low micromolar concentrations with experiment times under 10 min. This sensitivity is sufficient to assay competitive binding, but the concentration of protein places a lower limit on quantifiable K_i values of competitors. The throughput and sensitivity of this method could both be further improved with continued efforts toward probe ligand design.

■ ASSOCIATED CONTENT

Supporting Information

The Supporting Information is available free of charge at https://pubs.acs.org/doi/10.1021/acschembio.2c00566.

Supplementary data and figures from HSQC and CPMG NMR experiments, parameters from nonlinear regressions, descriptions of data analysis and equations, experimental methods, chemical synthesis procedures and characterization data, and NMR spectra (PDF)

■ AUTHOR INFORMATION

Corresponding Author

Kevan M. Shokat − *Department of Cellular and Molecular Pharmacology, University of California San Francisco, San Francisco, California 94158, United States; Howard Hughes Medical Institute, San Francisco, California 94158, United States;* orcid.org/0000-0001-8590-7741; Email: kevan.shokat@ucsf.edu

Authors

D. Matthew Peacock − *Department of Cellular and Molecular Pharmacology, University of California San Francisco, San Francisco, California 94158, United States;* orcid.org/0000-0001-8558-5535

Mark J. S. Kelly − *Department of Pharmaceutical Chemistry, University of California San Francisco, San Francisco, California 94158, United States;* orcid.org/0000-0003-3209-1018

Complete contact information is available at: https://pubs.acs.org/10.1021/acschembio.2c00566

Funding

D.M.P. is supported by a Ruth Kirschstein NRSA from the NCI of the NIH (F32CA253966). K.M.S. acknowledges support from the NIH (5R01CA244550), the Samuel Waxman Cancer Research Foundation, and HHMI. The content of this publication is solely the responsibility of the authors and does not necessarily represent the official views of the NIH.

Notes

The authors declare the following competing financial interest(s): K.M.S. is an inventor on patents owned by University of California San Francisco covering KRAS targeting small molecules licensed to Araxes and Erasca. K.M.S. has consulting agreements for the following companies, which involve monetary and/or stock compensation: Revolution Medicines, Black Diamond Therapeutics, BridGene Biosciences, Denali Therapeutics, Dice Molecules, eFFECTOR Therapeutics, Erasca, Genentech/Roche, Janssen Pharmaceuticals, Kumquat Biosciences, Kura Oncology, Mitokinin, Type6 Therapeutics, Venthera, Wellspring Biosciences (Araxes Pharma), Turning Point, Ikena, Initial Therapeutics, and BioTheryX.

■ ACKNOWLEDGMENTS

We thank Z. Zhang (UCSF) for his advice and donation of samples used in this work ($KRas^{G12D/T35S}$, TEV protease, RAF1-RBD 52-131, and KD2).

■ REFERENCES

(1) Prior, I. A.; Hood, F. E.; Hartley, J. L. The Frequency of Ras Mutations in Cancer. *Cancer Res.* **2020**, *80* (14), 2969−2974.

(2) Lu, S.; Jang, H.; Muratcioglu, S.; Gursoy, A.; Keskin, O.; Nussinov, R.; Zhang, J. Ras Conformational Ensembles, Allostery, and Signaling. *Chem. Rev.* **2016**, *116* (11), 6607−6665.

(3) Moore, A. R.; Rosenberg, S. C.; McCormick, F.; Malek, S. RAS-targeted therapies: is the undruggable drugged? *Nat. Rev. Drug Discov* **2020**, *19* (8), 533−552.

(4) Ostrem, J. M. L.; Shokat, K. M. Direct small-molecule inhibitors of KRAS: from structural insights to mechanism-based design. *Nat. Rev. Drug Discovery* **2016**, *15* (11), 771−785.

(5) Ostrem, J. M.; Peters, U.; Sos, M. L.; Wells, J. A.; Shokat, K. M. K-Ras(G12C) inhibitors allosterically control GTP affinity and effector interactions. *Nature* **2013**, *503* (7477), 548−551.

(6) Patricelli, M. P.; Janes, M. R.; Li, L.-S.; Hansen, R.; Peters, U.; Kessler, L. V.; Chen, Y.; Kucharski, J. M.; Feng, J.; Ely, T.; Chen, J. H.; Firdaus, S. J.; Babbar, A.; Ren, P.; Liu, Y. Selective Inhibition of Oncogenic KRAS Output with Small Molecules Targeting the Inactive State. *Cancer Discovery* **2016**, *6* (3), 316−329.

(7) Lito, P.; Solomon, M.; Li, L.-S.; Hansen, R.; Rosen, N. Allele-specific inhibitors inactivate mutant KRAS G12C by a trapping mechanism. *Science* **2016**, *351* (6273), 604−608.

(8) Janes, M. R.; Zhang, J.; Li, L.-S.; Hansen, R.; Peters, U.; Guo, X.; Chen, Y.; Babbar, A.; Firdaus, S. J.; Darjania, L.; Feng, J.; Chen, J. H.; Li, S.; Li, S.; Long, Y. O.; Thach, C.; Liu, Y.; Zarieh, A.; Ely, T.; Kucharski, J. M.; Kessler, L. V.; Wu, T.; Yu, K.; Wang, Y.; Yao, Y.; Deng, X.; Zarrinkar, P. P.; Brehmer, D.; Dhanak, D.; Lorenzi, M. V.; Hu-Lowe, D.; Patricelli, M. P.; Ren, P.; Liu, Y. Targeting KRAS Mutant Cancers with a Covalent G12C-Specific Inhibitor. *Cell* **2018**, *172* (3), 578−589.

(9) Hansen, R.; Peters, U.; Babbar, A.; Chen, Y.; Feng, J.; Janes, M. R.; Li, L.-S.; Ren, P.; Liu, Y.; Zarrinkar, P. P. The reactivity-driven biochemical mechanism of covalent KRASG12C inhibitors. *Nature Structural & Molecular Biology* **2018**, *25* (6), 454−462.

(10) Canon, J.; Rex, K.; Saiki, A. Y.; Mohr, C.; Cooke, K.; Bagal, D.; Gaida, K.; Holt, T.; Knutson, C. G.; Koppada, N.; Lanman, B. A.; Werner, J.; Rapaport, A. S.; San Miguel, T.; Ortiz, R.; Osgood, T.; Sun, J.-R.; Zhu, X.; McCarter, J. D.; Volak, L. P.; Houk, B. E.; Fakih, M. G.; O'Neil, B. H.; Price, T. J.; Falchook, G. S.; Desai, J.; Kuo, J.; Govindan, R.; Hong, D. S.; Ouyang, W.; Henary, H.; Arvedson, T.; Cee, V. J.; Lipford, J. R. The clinical KRAS(G12C) inhibitor AMG 510 drives anti-tumour immunity. *Nature* **2019**, *575* (7781), 217−223.

(11) Lanman, B. A.; Allen, J. R.; Allen, J. G.; Amegadzie, A. K.; Ashton, K. S.; Booker, S. K.; Chen, J. J.; Chen, N.; Frohn, M. J.; Goodman, G.; Kopecky, D. J.; Liu, L.; Lopez, P.; Low, J. D.; Ma, V.; Minatti, A. E.; Nguyen, T. T.; Nishimura, N.; Pickrell, A. J.; Reed, A. B.; Shin, Y.; Siegmund, A. C.; Tamayo, N. A.; Tegley, C. M.; Walton, M. C.; Wang, H.-L.; Wurz, R. P.; Xue, M.; Yang, K. C.; Achanta, P.; Bartberger, M. D.; Canon, J.; Hollis, L. S.; McCarter, J. D.; Mohr, C.; Rex, K.; Saiki, A. Y.; San Miguel, T.; Volak, L. P.; Wang, K. H.; Whittington, D. A.; Zech, S. G.; Lipford, J. R.; Cee, V. J. Discovery of a Covalent Inhibitor of KRASG12C (AMG 510) for the Treatment of Solid Tumors. *J. Med. Chem.* **2020**, *63* (1), 52−65.

(12) Molina-Arcas, M.; Samani, A.; Downward, J. Drugging the Undruggable: Advances on RAS Targeting in Cancer. *Genes* **2021**, *12* (6), 899.

(13) Fell, J. B.; Fischer, J. P.; Baer, B. R.; Blake, J. F.; Bouhana, K.; Briere, D. M.; Brown, K. D.; Burgess, L. E.; Burns, A. C.; Burkard, M.

R.; Chiang, H.; Chicarelli, M. J.; Cook, A. W.; Gaudino, J. J.; Hallin, J.; Hanson, L.; Hartley, D. P.; Hicken, E. J.; Hingorani, G. P.; Hinklin, R. J.; Mejia, M. J.; Olson, P.; Otten, J. N.; Rhodes, S. P.; Rodriguez, M. E.; Savechenkov, P.; Smith, D. J.; Sudhakar, N.; Sullivan, F. X.; Tang, T. P.; Vigers, G. P.; Wollenberg, L.; Christensen, J. G.; Marx, M. A. Identification of the Clinical Development Candidate MRTX849, a Covalent KRASG12C Inhibitor for the Treatment of Cancer. *J. Med. Chem.* **2020**, *63* (13), 6679−6693.

(14) Wang, X.; Allen, S.; Blake, J. F.; Bowcut, V.; Briere, D. M.; Calinisan, A.; Dahlke, J. R.; Fell, J. B.; Fischer, J. P.; Gunn, R. J.; Hallin, J.; Laguer, J.; Lawson, J. D.; Medwid, J.; Newhouse, B.; Nguyen, P.; O'Leary, J. M.; Olson, P.; Pajk, S.; Rahbaek, L.; Rodriguez, M.; Smith, C. R.; Tang, T. P.; Thomas, N. C.; Vanderpool, D.; Vigers, G. P.; Christensen, J. G.; Marx, M. A. Identification of MRTX1133, a Noncovalent, Potent, and Selective KRASG12D Inhibitor. *J. Med. Chem.* **2022**, *65* (4), 3123−3133.

(15) Pellecchia, M.; Sem, D. S.; Wüthrich, K. Nmr in drug discovery. *Nat. Rev. Drug Discovery* **2002**, *1* (3), 211−219.

(16) Maurer, T.; Garrenton, L. S.; Oh, A.; Pitts, K.; Anderson, D. J.; Skelton, N. J.; Fauber, B. P.; Pan, B.; Malek, S.; Stokoe, D.; Ludlam, M. J. C.; Bowman, K. K.; Wu, J.; Giannetti, A. M.; Starovasnik, M. A.; Mellman, I.; Jackson, P. K.; Rudolph, J.; Wang, W.; Fang, G. Small-molecule ligands bind to a distinct pocket in Ras and inhibit SOS-mediated nucleotide exchange activity. *Proc. Natl. Acad. Sci. U. S. A.* **2012**, *109* (14), 5299−5304.

(17) Sun, Q.; Burke, J. P.; Phan, J.; Burns, M. C.; Olejniczak, E. T.; Waterson, A. G.; Lee, T.; Rossanese, O. W.; Fesik, S. W. Discovery of Small Molecules that Bind to K-Ras and Inhibit Sos-Mediated Activation. *Angew. Chem., Int. Ed.* **2012**, *51* (25), 6140−6143.

(18) Smith, M. J.; Neel, B. G.; Ikura, M. NMR-based functional profiling of RASopathies and oncogenic RAS mutations. *Proc. Natl. Acad. Sci. U. S. A.* **2013**, *110* (12), 4574−4579.

(19) Zhao, Q.; Fujimiya, R.; Kubo, S.; Marshall, C. B.; Ikura, M.; Shimada, I.; Nishida, N. Real-Time In-Cell NMR Reveals the Intracellular Modulation of GTP-Bound Levels of RAS. *Cell Reports* **2020**, *32* (8), 108074.

(20) Marshall, C. B.; Meiri, D.; Smith, M. J.; Mazhab-Jafari, M. T.; Gasmi-Seabrook, G. M. C.; Rottapel, R.; Stambolic, V.; Ikura, M. Probing the GTPase cycle with real-time NMR: GAP and GEF activities in cell extracts. *Methods* **2012**, *57* (4), 473−485.

(21) Vasta, J. D.; Peacock, D. M.; Zheng, Q.; Walker, J. A.; Zhang, Z.; Zimprich, C. A.; Thomas, M. R.; Beck, M. T.; Binkowski, B. F.; Corona, C. R.; Robers, M. B.; Shokat, K. M. KRAS is vulnerable to reversible switch-II pocket engagement in cells. *Nat. Chem. Biol.* **2022**, *18* (6), 596−604.

(22) Gentile, D. R.; Rathinaswamy, M. K.; Jenkins, M. L.; Moss, S. M.; Siempelkamp, B. D.; Renslo, A. R.; Burke, J. E.; Shokat, K. M. Ras Binder Induces a Modified Switch-II Pocket in GTP and GDP States. *Cell Chemical Biology* **2017**, *24* (12), 1455−1466.

(23) Buchholz, C. R.; Pomerantz, W. C. K. 19F NMR viewed through two different lenses: ligand-observed and protein-observed 19F NMR applications for fragment-based drug discovery. *RSC Chemical Biology* **2021**, *2* (5), 1312−1330.

(24) Dalvit, C.; Fagerness, P. E.; Hadden, D. T. A.; Sarver, R. W.; Stockman, B. J. Fluorine-NMR Experiments for High-Throughput Screening: Theoretical Aspects, Practical Considerations, and Range of Applicability. *J. Am. Chem. Soc.* **2003**, *125* (25), 7696−7703.

(25) Dalvit, C.; Vulpetti, A. Ligand-Based Fluorine NMR Screening: Principles and Applications in Drug Discovery Projects. *J. Med. Chem.* **2019**, *62* (5), 2218−2244.

(26) Awad, M. M.; Liu, S.; Rybkin, I. I.; Arbour, K. C.; Dilly, J.; Zhu, V. W.; Johnson, M. L.; Heist, R. S.; Patil, T.; Riely, G. J.; Jacobson, J. O.; Yang, X.; Persky, N. S.; Root, D. E.; Lowder, K. E.; Feng, H.; Zhang, S. S.; Haigis, K. M.; Hung, Y. P.; Sholl, L. M.; Wolpin, B. M.; Wiese, J.; Christiansen, J.; Lee, J.; Schrock, A. B.; Lim, L. P.; Garg, K.; Li, M.; Engstrom, L. D.; Waters, L.; Lawson, J. D.; Olson, P.; Lito, P.; Ou, S.-H. I.; Christensen, J. G.; Jänne, P. A.; Aguirre, A. J. Acquired Resistance to KRASG12C Inhibition in Cancer. *New England Journal of Medicine* **2021**, *384* (25), 2382−2393.

(27) Zhang, Z.; Gao, R.; Hu, Q.; Peacock, H.; Peacock, D. M.; Dai, S.; Shokat, K. M.; Suga, H. GTP-State-Selective Cyclic Peptide Ligands of K-Ras(G12D) Block Its Interaction with Raf. *ACS Central Science* **2020**, *6* (10), 1753−1761.

https://doi.org/10.1021/acschembio.2c00566
ACS Chem. Biol. 2022, 17, 2710−2715